9th ECCOMAS Thematic Conference on the Mechanical Response of Composites
COMPOSITES 2023
G. Catalanotti, H. Petterman and G. Pittaresi (Eds)

INVESTIGATION INTO THE MANUFACTURE OF HYBRID WEAR RESISTANT FORGING TOOLS USING TAILORED FORMING TECHNOLOGY

M. Till*, J. Siring, H. Wester, J. Peddinghaus, J. Uhe and K. Brunotte

Institute of Forming Technology and Machines, Leibniz Universität Hannover
An der Universität 2, 30823 Garbsen, Germany
* till@ifum.uni-hannover.de

Keywords: Tailored Forming, Wear resistance, Thermo mechanical loads

Summary: *Forging tools that are subject to high thermo-mechanical loads require a correspondingly high heat resistance, hardness and ductility to prevent undesirable failure patterns due to wear, plastic deformation and crack formation. These properties are mainly required in the layer of the tool engraving close to the surface, as this area is exposed to the highest loads due to the contact with the hot workpiece. With the heat transfer from the workpiece to the tool, a cyclic tempering process of the tool material often occurs in this area, resulting in a decrease in wear resistance. Diffusion treatments of the tool surface, such as additional nitriding, cannot provide sufficient protection in thermally highly stressed tool areas, as the heat-affected zone in these areas extends beyond the surface modification. As a result, a tempered layer forms under the nitrided layer, on which it can slide off or break as a result of the high process loads and the wear protection is lost. The use of nickel-based alloys promises an improvement in service life due to their high specific heat. However, these alloys are much more expensive than hot-work tool steels and are more difficult to machine, which has a negative effect on the economic use as a die material. Furthermore, nickel-based alloys do not have the high strength of steel that is often required in the base material that is subject to low thermal loads.*

To reduce the material usage of nickel-based alloys, but to fully take advantage of their positive properties, the suitability of the Tailored Forming concept in thermo-mechanically highly stressed areas were investigated within the scope of this research. For this reason, hybrid forging tool inserts with a base material of hot-work tool steel and a protective nickel-based alloy surface layer were produced. The hybrid tools are manufactured through a process combination of rotatory friction welding and die forging. The surface enlargement as a result of the forming process is to be used specifically to protect the relevant tool areas with a layer of nickel-based alloy and at the same time minimize the use of the expensive material. The effects of the thermo mechanical treatments occurring in the joining zone were examined and the potential of the technology was investigated.

1 INTRODUCTION

Forging enables a material-efficient production and is used for the preform manufacturing of dynamically loaded components. The number of forming operations during which a die can be used without failure is defined as the service life. This depends in particular on the thermomechanical and tribological loads during forming, the material properties of the die material and the design of the die engraving [1]. The mechanical stresses increase as the forging or the dynamic pressure progresses and reach their maximum at the end of the forming process [2]. The temperature peak of the forging cycle is also at this point, which leads to a maximum of the load spectrum. Subsequently, the die surface cools rapidly as soon as the die is opened. After removal of the workpiece, the lubricant is applied for the next forging process, which causes additional edge zone cooling to a value below the base temperature of the die. The tools for these forging operations are subject to high thermomechanical stresses and require high-temperature strength, hardness and elasticity to prevent early material failure. These properties are particularly necessary in the layer of the tool contour close to the surface, as this area is exposed to the highest loads. While forging, the surface temperature fluctuates cyclically between the condition after spray-cooling of 150 °C - 350 °C and the temperature peak at the end of forming at approx. 700 °C [3]. This results in a non-stationary (locally and temporally variable) and highly dynamic temperature field due to the process [4]. In industrial processes, cycle times of 0.4 s can be achieved. The resulting short thermal load times add up, causing a tempering effect. The highest temperatures while forging occur in radii and complex contours of the dies, where heat spots can build up, limiting the achievable service life.
A significant part of the unit costs of forged components results from the tool production and the production interruptions for tool change after the occurrence of failure [5]. The resulting production costs depend up to 10 % on the tools and their service life [6]. Here, material-related process limits occur, which are determined by the ratio of strength to ductility as a function of temperature [7]. Typical damage mechanisms that can lead to tool failure (cf. Figure 1) are wear (abrasion, adhesion), mechanical and thermal cracking (due to thermal shock) and plastic deformation [8]. By avoiding wear through local optimisation of the tool edge layer, the service life can be increased and consequently the costs significantly reduced.

Overheating, thermal overload	Thermal shock	Abrasion, adhesion
- Loss of base hardness - Plastic deformation	- Crack formation - Breakouts - Tool breakage	- Material removal - Material adhesion

Figure 1: Typical damage mechanisms in forging tools leading to tool failure [8].

Various approaches exist to increase the resistance of forging tools to such damages. One approach is to reduce the tool load during the forming process and thus increase the service life. The other is to modify the tool surface and adapt it to the types of stress. Thermal [9] and thermochemical surface treatments [10] of hot work tool steels as well as the application of wear-resistant hard material coatings [11] have proven to be economical methods for increasing tool life. Due to the small zone of influence ($< 500\ \mu$m) of these surface treatments, the thermal application limits of hot-work tool steels cannot be significantly extended. The modified surface layer does not withstand continuous stress since the material behaviour of the base material is strongly deviating, especially at high thermal loads. Resulting tempering effects below the modified layer ultimately leads to a high strength and hardness gradient, which is one of the most frequent causes of failure. Nickel-based alloys show their advantages in the high-temperature range, where they can far surpass common hot-work tool steels in their hot strength. Due to the high material costs, these alloys have hardly been used in practice [12]. Previous applications of nickel-based alloys have been aimed at mono-material use and are limited by its high costs [13]. Furthermore, this material shows poorer strength and hardness properties than steel at low temperatures, which is why it is mechanically not useful for the production of tools that are predominantly exposed to low thermal loads. To use the advantages of nickel-based alloys efficiently, its material use must therefore be reduced through local integration and the surface layer properties must be improved for use in the low-temperature range. In this context, Tailored Forming enables load-efficient material application and simultaneous improvement of the microstructural properties through forming hybrid pre-joined semi-finished products [14].

2 METHODS AND MATERIALS

The objective of this research is to develop and analyse a process route for the production of hybrid tools with high resistance to thermo-mechanically induced failure patterns. For this purpose, surface enlargement during forging is used to coat the base material of hot work steel with a protective layer of high-temperature resistant nickel-based alloy in highly stress exposed areas of the tool. Since the materials show different flow behaviour, which is highly dependent on temperature and forming speed, a general formability of the joined materials and the in-process surface modification are to be demonstrated. The concept for the applied process is shown in Figure 2. The hot-work tool steel X38CrMoV5-1 (AISI H11) is used for the high-volume base material and the nickel-based alloy NiCr22Mo9Nb (Alloy 625) for the engraving surface layer. To adjust the nickel-based alloy distribution in the surface layer of the formed component, Alloy 625 must first be applied through a defined layer height in the semi-finished product. For the pre-joining process, friction welding with a Kuka Genius Plus is used. The friction welded semi-finished products with a diameter of 40 mm are machined to a total height of 50 mm and the investigated of the nickel-based alloy thicknesses (IH) of 3 mm and 10 mm. To find a suitable combination for the hybrid semi-finished products with a defect free joining zone, upsetting and frictional pressure are varied during friction welding with transferred parameters from studies according to Cheepu et al. [15]. The friction welded parts are tested in a metallographic analysis and hardness measurements of the joining zone. In the following process step, numerical simulations were carried out next to the experimental investigation to quantify the resulting local effective plastic strain distribution within the formed die inserts for both *IH*. A 3D model was created in the commercial FE system Simufact Forming 16.0 using previously determined material data. Jia et al. describes that the optimum process parameters for forming Alloy 625 are 1100 - 1200 °C and low strain rates of 1 - 10 s-1, at which the perfect dynamic recrystallization occurs and a fine grain structure is obtained [16]. Therefore, a forming temperature of 1100 °C and a press speed of 30 mm/s was investigated. The parts were heated and subsequently formed on a hydraulic press with the tool geometry shown in Figure 2. After forming, the workpieces are cooled with water applied to the Alloy 625 side, to avoid cracks in the tool steel due to different thermal expansion and conductivity of the materials. The formed cups are analysed microscopically to examine the joining zone for defects and to evaluate the microstructure after forming, while the corresponding properties are investigated in hardness test and compared to the simulation results. Further diffusion and heat treatments to increase the hardness of the die surfaces are not part of this investigation.

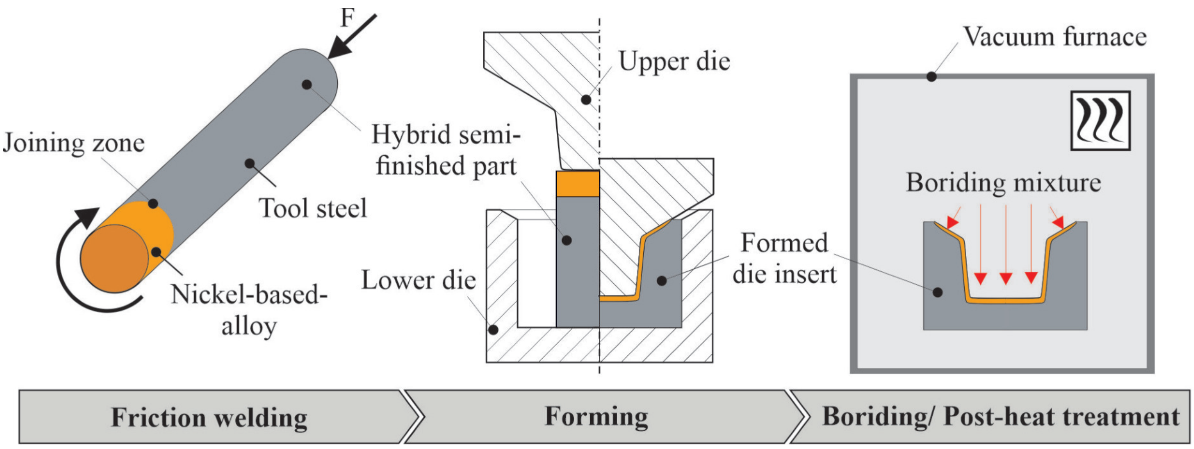

Figure 2: Scheme of the production of wear-resistant hybrid tools by Tailored Forming.

3 RESULTS

By varying the friction welding parameters, the hardness values in the joining zone are influenced, see Figure 3 (left). As the upsetting pressure increases, the hardness in the joining zone and also both materials rise slightly, resulting from forming-induced hardening. However, no significant influence of the frictional pressure could be detected. For all parameter combinations of frictional and upsetting pressure that were investigated, it was possible to produce suitable joint connections. Furthermore, images in the cross-section of the friction welded parts are shown in Figure 3 (right). Swirled layers occur in the centre of the joining zone which increase the surface contact and lead to an interlocking of the materials. At lower upsetting pressures, a characteristic circumferential uncontacted area occurs in the outer area of the joining zone. The material flow is decisively dependent on the frictional heat generated and the resulting plasticity of the materials. In the outer area, more energy and thus heat is introduced due to the high relative movement during friction welding. With increasing upsetting force, a movement of the defect into the outer area can be observed. This defect can be reduced or removed by a higher upsetting pressure with a stronger lateral material displacement and a larger welding flash.

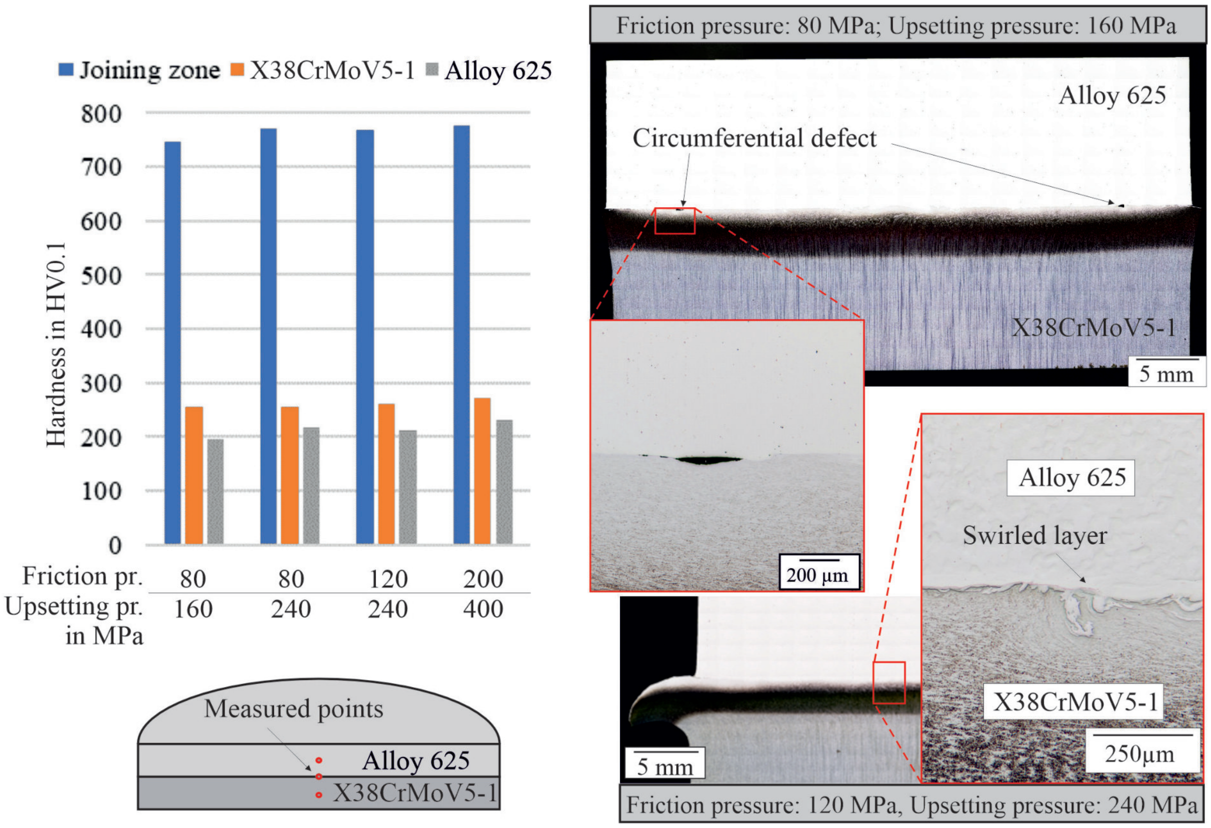

Figure 3: Hardness comparison in the joining zone (left) and images in cross-section after friction welding with different friction and upsetting pressures (right).

The hardness profile (step width: 0.5 mm) of a friction-welded X38CrMoV5-1/ Alloy 625-specimen with the highest parameter set of 200 MPa friction pressure and 400 MPa upsetting pressure is shown in Figure 4. It can be seen that there is hardly any deformation on the Alloy 625 side and no increase in hardness. A distinction between the heat-affected zone (HAZ) of the steel and the thermo-mechanically affected zone (TMAZ) manifested itself in the microstructure. The HAZ is caused by the applied frictional heat, which leads to austenitisation with subsequent hardening of the steel while cooling. The TMAZ near the joining zone is plastically deformed, causing an additional increase in hardness due to higher dislocation density and grain refinement. In the HAZ, the hardness rises up to 600 HV0.1. In the TMAZ, the hardness increases further to almost 800 HV0.1. With the friction welding parameters applied, these zones have a combined width of approximately 3 mm.

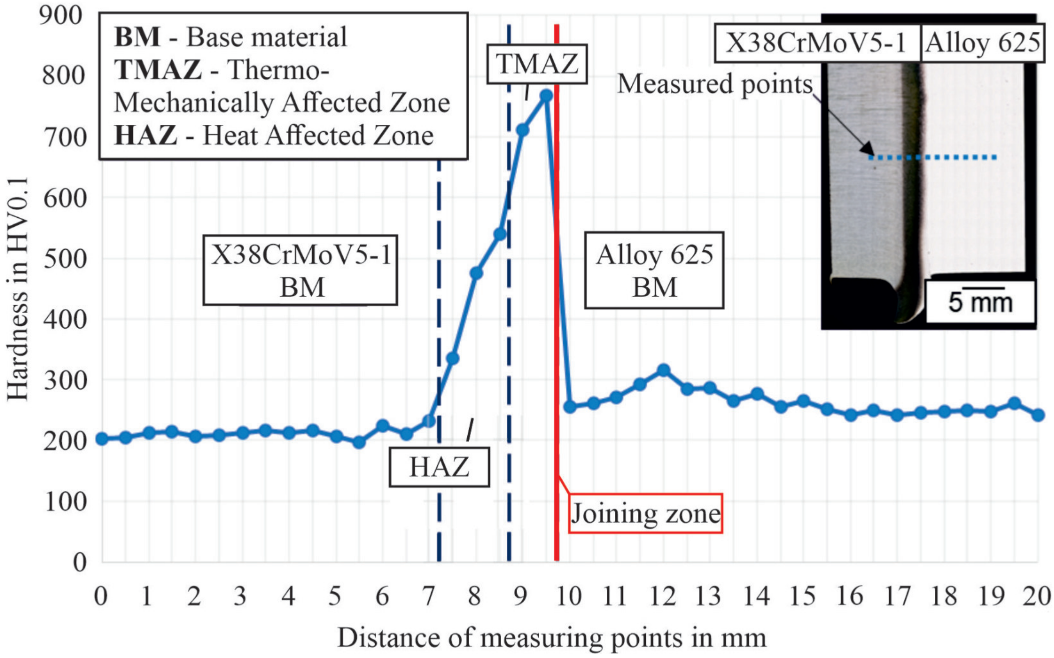

Figure 4: Hardness measurement of a friction-welded steel-Alloy 625 semi-finished product.

The final material distribution was analysed with the help of the FE-simulation in order to define an initial *IH* (cf. Figure 5). The same boundary conditions, like stroke, forming temperature and geometry were chosen for the simulation as for the experiments. While the material is located inside the cup with an *IH* of 3 mm, it overlaps the upper cup area with an *IH* of 10 mm. The reduction of the Inconel layer thickness results in a strong thinning of Alloy 625 down to a few μm, without delamination or breaking. However, no sufficient Alloy 625 layer remains for the subsequent diffusion and thermal post-treatment, which could form a sufficient diffusion layer above the joining zone. In addition, the thermal behaviour of the two materials differs significantly, which could have a negative effect on the alternating loads in service. Achieving a sufficient layer thickness is necessary for post-processing and later application, therefore a layer thickness of 10 mm was chosen for further experimental tests. When comparing the results of the effective plastic strain for the two *IH*, a difference in the maximum values can be seen. The lower *IH* shows a maximum effective plastic strain of almost 9.0 in the area of the greatest thickness reduction of the Alloy 625. At the higher starting height, the maximum effective plastic strain reduces to 4.0. The effective plastic strain distribution was in the same range for both variants. It can be seen that the most of the deformation took place within the steel. In both cases, a conical dead zone without plastic deformation is created in the bottom area which can be attributed to the stress distribution during forming and occurs independently of the material.

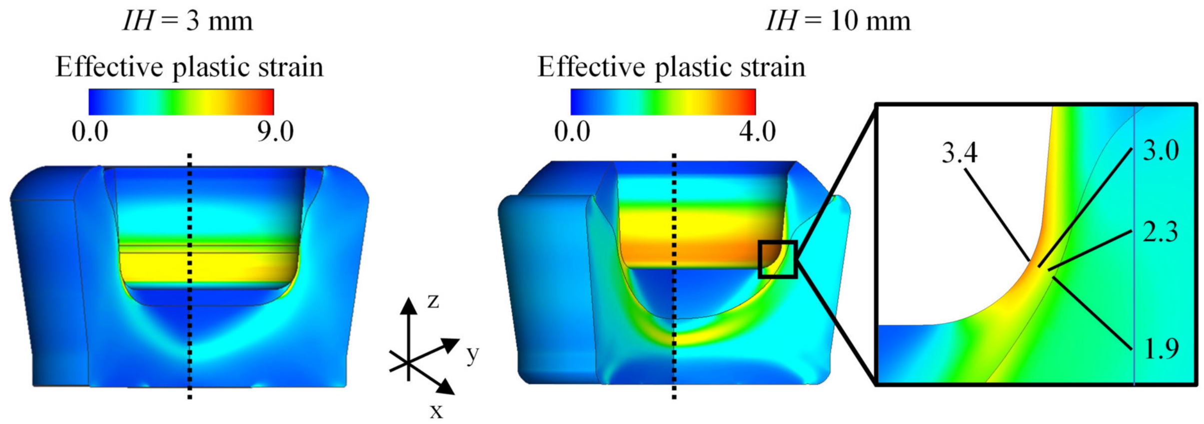

Figure 5: Overview result of the effective plastic strain of both initial heights for Alloy 625 at a forming temperature of 1000 °C and a speed of 15 mm/s.

After the numerical investigation, the friction-welded specimens were used to form die inserts (e. g. Figure 2). With two semi-finished variations of *IH* the joint was formed without material failure, see Figure 6. The comparison with the simulation in Figure 5 shows that these are geometrically identical to the formed components. While the material is located inside the cup with an *IH* of 3 mm, it overlaps the upper cup area with an *IH* of 10 mm. The reduction of the Alloy 625-layer thickness results in a strong thinning of the Alloy 625 down to a few μm and thus an uneven distribution, but no delamination or tearing of the material. However, no sufficient Alloy 625 layer remains for the subsequent diffusion and thermal post-treatment, which could form a sufficient diffusion layer above the joining zone. In addition, the thermal behaviour of the two materials differs significantly, which could have a negative effect on the alternating loads in service. Obtaining a sufficient layer thickness thus appears to be necessary for post-processing and later application.

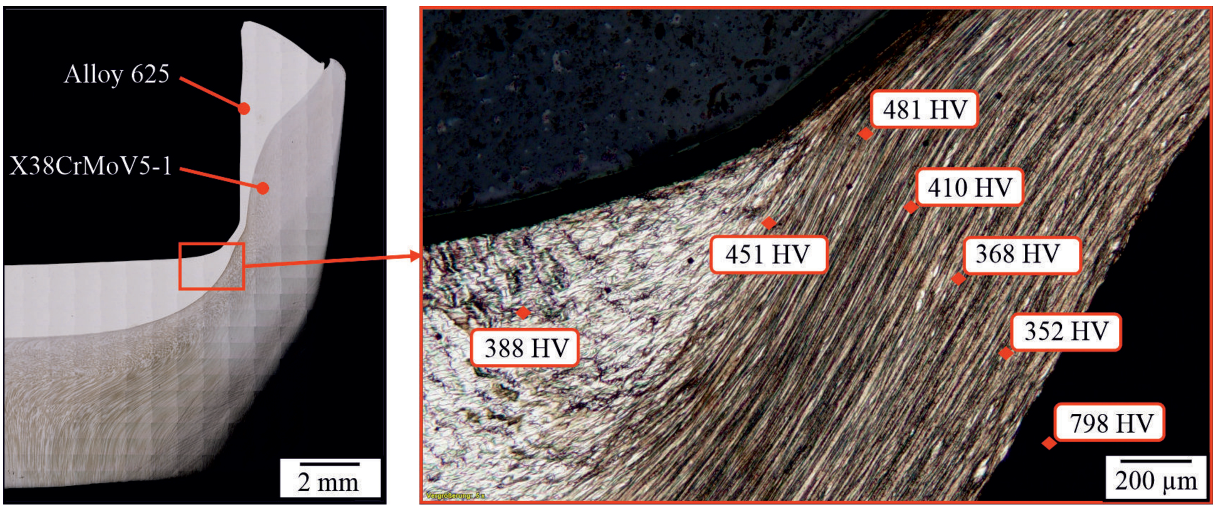

Figure 6: Hardness values at the radius of a friction welded and formed component with an *IH* = 10 mm, T_f = 1100 °C.

The Alloy 625 microstructure and the measured hardness at the inner radius of the component is shown in Figure 6. The hardness values on the Alloy 625 side orthogonal to the radius decrease steadily from 481 HV0.1 near the surface to 352 HV0.1 near the joining zone. The areas close to the component surface experience a stronger strain hardening which is also indicated by the local distribution of effective plastic strain, cf. Figure 5. In the central bottom area, where only low deformation takes place, the measured hardness is 388 HV0.1 and increases towards the radius. For the steel side, a hardness value of 798 HV0.1 was determined near the joining zone. Consequently, there is a high hardness gradient at the transition from nickel-based alloy to steel.

The hardness measurements shown in Figure 7 (left) were carried out along the radius in 0.5 mm steps on the Alloy 625 side with die inserts formed at temperatures $T_f = 1000$ °C and 1100 °C. The measurements start at the bottom part and run along the radius. Initially, the hardness of the Alloy 625 at $T_f = 1000$ °C is approx. 400 HV0.1 and increases to over 500 HV0.1 along the radius. The part formed at 1100 °C shows also a hardness increase in the radius, but this is approx. 100 HV0.1 lower than the hardness achieved at $T_f = 1000$°C. The reason for this is the strain hardening of the Alloy 625 due to the lower forming temperature. In addition, grain refinement is achieved in Alloy 625 during recrystallisation at temperatures below approx. 1050 °C [13]. The hardness values of the steel were determined at the radius orthogonal to the surface in 0,3 mm distance, see Figure 7 (right). The hardness curves of the X38CrMoV5-1 show a significantly greater discrepancy of 270 HV0.1 between the two forming temperatures. At $T_f = 1100$ °C an average hardness of 821 HV0.1 is achieved in the steel. This value drops to 554 HV0.1 at $T_f = 1000$ °C. Thus, the hardness gradient between the two materials is significantly higher at $T_f = 1100$ °C with over 400 HV0.1. In contrast, the gradient at $T_f = 1000$ °C is only 70 HV0.1.

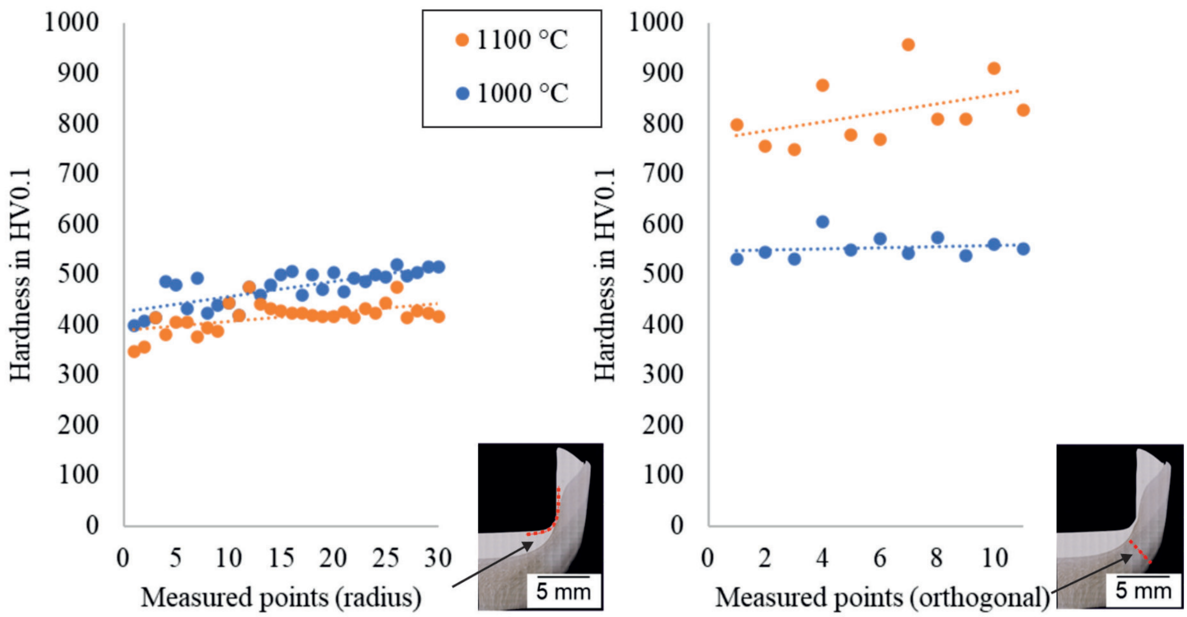

Figure 7: Hardness of the Alloy 625 layer along the inner radius (left) and in the direction perpendicular to the radius for X38CrMoV5-1 (right) at a forming temperature of 1000 °C and 1100 °C respectively.

Since the values in the Alloy 625 are locally very different, the hardness gradient also varies selectively. In Alloy 625, hardness values of 527 HV0.1 can be achieved at T_f = 1000 °C, whereas the steel can be 530 HV0.1. Therefore, with lower forming temperatures, the hardness gradient can be adjusted and optimised. The reason for the large difference in hardness of the tool steel due to the variation of the temperature can be attributed to the austenitisation temperature Ac3 of X38CrMoV5-1, which is approx. 1020 °C. The forming temperature of 1100 °C results in complete austenitisation of the steel and thus a higher martensite content in the quenched part.

In the Alloy 625-layer, significant differences in hardness result from the nonuniform distribution of the effective plastic strain (cf. Figure 5). The reached hardnessis below the common values for forging dies made of hot-work tool steel. For wear protection, a hardening of the edge layer is necessary. Therefore, the Alloy 625 surface must be borided after forming, which in turn requires post-hardening of the steel. After these treatments, the influence of the respective initial condition must be further investigated. It is still unknown how the correlating strength gradients affect the thermal behaviour of the joining zone during the heat treatment and in the later application of the die insert. After forming, the materials show zones with different grain sizes, which indicate the influence of the local effective plastic strain, the tool contact time and the thermal conductivity of both materials on the forming behaviour (cf. Figure 8).

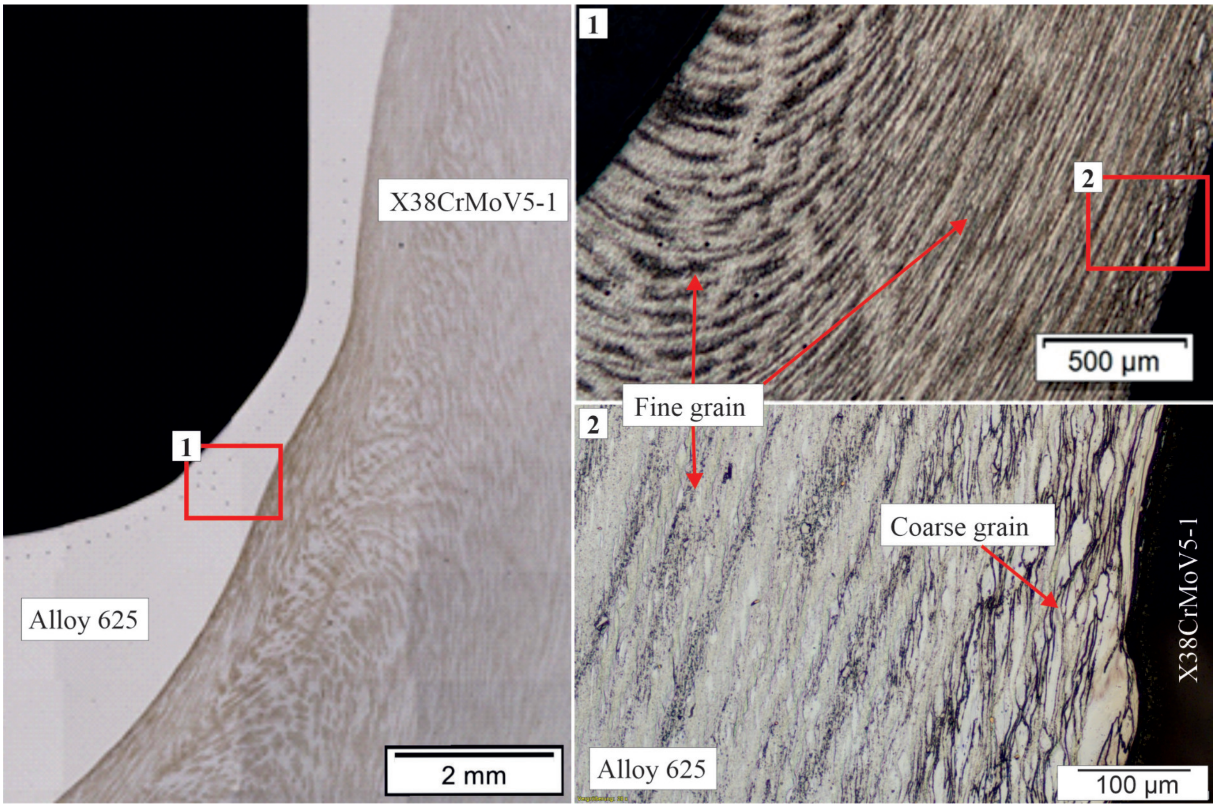

Figure 8: Flow behaviour of the materials in the radius area (formed with IH = 10 mm, T_f = 1100 °C).

The microscopic image of the inner radius of a sample that was formed with IH = 10 mm shows a coarse grain on the Alloy 625 side in the area of the joining zone correlating with the simulation results (cf. Figure 5). It indicates that hardly any material movement occurred in the nickel-based alloy close to the joining zone. However, despite the high deformation in this area, the joining zone does not show any cracks or carry-over of defects introduced during forming. Furthermore, the HAZ after joining shows no negative influence on the microstructure of the steel while forming. This could be due to austenitisation prior to forming. The different forming behaviour caused by the tool contact, may require individual cooling lubricant application and tool temperature control. Nevertheless, the pressure contact time with the tool cannot be further reduced due to the required slow forming speed of the Alloy 625.

4 CONCLUSIONS

This study investigated forming of friction welded Alloy 625 and X38CrMoV5-1 for the efficient material utilisation in forging tools. The comparison of the numerical analysis with the experimental tests shows a high geometric accuracy. It appears that in hybrid forming, the deformations introduced are mainly in the steel and Alloy 625 is almost not deformed, except in narrowed areas. Despite the non-uniform deformation behaviour, no delamination occurs, which indicates a high bond quality and general suitability for forming of pre-joined semi-finished products. The results show that the joining zone between Alloy 625 and X38CrMoV5-1 can be formed defect-free to the geometric requirements of the tool despite high effective plastic strain and high temperature gradients. Even with an initially high hardness in the TMAZ and HAZ, it was possible to form at 1000 °C and 1100 °C. The temperature shows a considerable influence on the final hardness and the material flow of both materials. The temperature dependence of the materials hardening effects play a decisive role in hybrid forming, which is why heat loss should be prevented by short transfer and tool contact times. However, the slow forming speed required on the Alloy 625 side prevents short tool contact. It was shown that a low $IH = 3$ mm leads to excessive thinning of the Alloy 625, which means that these die inserts cannot be further borided, heat treated and used in service life tests as the joining zone is too close to the surface. In further investigations, hybrid semi-finished parts made of non-hardenable Alloy 625 and hardenable Alloy 718 friction welded with tool steel are to be tested in a surface treatment by boriding with simultaneous ageing to investigate the influence of the base hardness on wear resistance. Furthermore, it will be examined how the subsequent heat treatments affect the material behaviour of the hybrid workpieces. To investigate the application properties in thermo-mechanically highly stressed engraving areas and if cyclic thermomechanical stresses on the joining zone should be avoided, serial forging tests are carried out with formed die inserts. From this, design recommendations for hybrid tools with consideration of the thermal load depth can be derived and transferred to different die geometries.

5 ACKNOWLEDGEMENTS

This study was funded by the Deutsche Forschungsgemeinschaft (DFG, German Research Foundation) - CRC 1153 - 252662854, transfer project T03. The authors gratefully acknowledge DFG's financial support.

REFERENCES

[1] E. Doege, G. Dreyer, S. Ruesch, Metal Forming: Close Die Forging. *Encyclopedia of materials*, 5390–5394, 2001.

[2] B.-A. Behrens, A. Huskic, D. Rosenbusch, J. Peddinghaus, H. Wester, M. Siegmund, J. Giedenbacher, J. Siring, Design, Characterisation and Numerical Investigations of Additively Manufactured H10 Hybrid-Forging Dies with Conformal Cooling Channels. *Metals 2022*, **12(7)**, 1063, 2022.

[3] O. Barrau, C. Boher, R. Gras, F. Rezai-Aria, Analysis of the friction and wear behaviour of hot work tool steel for forging. *Wear 255*, **7-12**, 1444–1454, 2003.

[4] H. Paschke, T. Yilkiran, L. Lippold, K. Brunotte, M. Weber, G. Braeuer, B.-A. Behrens: Adapted surface properties of hot forging tools using plasma technology for an effective wear reduction. *Wear 330-331*, 429 – 438, 2015.

[5] A. Alessio, D. Antonelli, R. Doglione, G. Genta, Die wear reduction by multifactorial Design of Experiments applied to forging simulations. *Procedia CIRP*, **112**, 424-429, 2022.

[6] K. Brüggemann, Methoden des Qualitätsmanagements beim Gesenkschmieden. *Dissertation*, Hannover, 1997.

[7] B.-A. Behrens, K. Brunotte, T. Petersen, R. Relge, M. Till, Transfer of ausforming parameters to scaled forging tools. *Proceedings 30th Anniversary International Conference on Metallurgy and Materials*, Brno, Czech Republic, 247-252, 2021.

[8] D. Heinemeyer, Untersuchungen zur Frage der Haltbarkeit von Schmiedegesenken. *Dissertation*, Hannover, 1976.

[9] K.-T. Rie, Recent advances in plasma diffusion processes. *Surface & coatings technology 112*, **1-3**, 56–62, 1999.

[10] J. Smolik, J. Walkowicz, J. Tacikowski, Influence of the structure of the composite: 'nitrided layer/PVD coating' on the durability of tools for hot working. *Surface and Coatings Technology 125*, **1-3**, 134–140, 2000.

[11] T. Yilkiran, B. A. Behrens, H. Paschke, M. Weber, H. Brand, The potential of plasma deposition techniques in the application field of forging processes. *Archives of Civil and Mechanical Engineering 12*, **3**, 284–291, 2012.

[12] J. R. Davis, Heat-resistant materials. *ASM Internat.*, **2**, Materials Park, Ohio, 1999.

[13] F. Klocke, Zerspanung mit geometrisch bestimmter Schneide. **9**, *Springer Vieweg*, Berlin, 2018.

[14] B.-A. Behrens, A. Chugreeva, J. Diefenbach, C. Kahra, S. Herbst, F. Nürnberger, H. J. Maier, Microstructural Evolution and Mechanical Properties of Hybrid Bevel Gears Manufactured by Tailored Forming. *Metals 2020*, **10(10)**, 1365, 2020.

[15] M. Cheepu, W. S. Che, Characterization of Interfacial Microstructure in Friction Welds Between Inconel 718 and SM45C Steel. *The Indian Institute of Metals*, **73 (6)**, 1567-1571, 2020.

[16] Z. Jia, Z. X. Gao, J. J. Ji, D.X. Liu, T.B. Guo, Y.T. Ding, High-temperature deformation behavior and processing map of the as-cast Inconel 625 alloy. *Rare Metals*, **40**, 2083-2091, 2020.